Applied Physics A (2019) 125:291
https://doi.org/10.1007/s00339-019-2600-2

Applied Physics A
Materials Science & Processing

Check for updates

Fabrication of microfluidic channels with various cross-sectional shapes using anisotropic etching of Si and self-alignment

Dong-Ki Lee[1] · Joo Yong Kwon[2] · Young Hak Cho[2]

Received: 30 December 2018 / Accepted: 30 March 2019 / Published online: 3 April 2019

Abstract

A novel and simple fabrication method was proposed to produce microfluidic channels with various cross-sectional shapes, such as parallelogram, rhombus, pentagon and hexagon. The present study has the advantages of not only fabricating the microfluidic channel shapes that have not been reported before, but also the fabrication process is simple, flexible and robust. Microfluidic channels were fabricated using anisotropic wet etching of Si wafer and self-alignment between Si structure and PDMS mold. In this regard, (100) single crystal Si wafer was used to fabricate the Si microchannel and the master for PDMS mold using photolithography and anisotropic KOH etching. The Si structure for the microchannel and master were formed from the same Si wafer by KOH etching, and the PDMS mold was made from the Si master. Finally, the microchannels with various cross-sectional shapes could be easily formed through self-alignment of the Si microchannel and PDMS mold. They were permanently bonded using O_2 plasma treatment. It is expected that the fabricated microchannel with various cross-sectional shapes can be used in wide fields such as heat transfer, microscale transport of particle and fluid, and particle separation based on inertial focusing.

1 Introduction

Over the last 2 decades, the microfluidic technique has experienced wide expansion of its applications in a vast range of fields, such as microelectronic cooling, MEMS (microelectromechanical systems), fuel cell technology, micro reactors for cell biology and tissue engineering, and medical and biomedical devices. Many microfluidic devices were easily fabricated through replica molding process of polydimethylsiloxane (PDMS) after the standard ultra-violet (UV) photolithography process [1]. However, the cross-sectional shapes of the microchannels fabricated through photolithography and micromolding are restricted to squares and rectangles due to the micromolds with vertical sidewalls. Furthermore, some microfluidic devices were also fabricated through hot-embossing or micro-injection molding process using thermoplastic polymers, such as poly (methylmethacrylate) (PMMA), cyclic olefin copolymer (COC), and polycarbonate (PC) [2, 3]. In this case, the cross-sectional shapes of the microchannels were determined by a metal mold whose fabrication technique is high-cost and time-consuming.

Some groups conducted theoretical investigations on microchannels with cross-sections such as circle, rhombus, pentagon and hexagon [4–6]. Tamayol et al. [4, 5] presented analytical solutions for laminar fully developed flow and fully developed pressure-driven slip-flow inside microchannels with noncircular cross-section. Sadeghi et al. [6] analyzed fully developed electroosmotic flow in hydrophobic microchannels with general cross-section. However, they could not present the experimental results due to difficulties in fabrication of microchannels with various cross-sectional shapes. To understand various physical and chemical phenomena within microchannels with various cross-sectional shapes comparison of both the theoretical and experimental results is necessary. In this regard, it is important to develop a simple and novel fabrication method of microchannels with various cross-sectional shapes.

The recent improvements in the microfabrication technique have made fabrication of microchannels with non-rectangular cross-sections, such as circle, half-circle, triangle and trapezoid possible [7–14]. Some researchers made

✉ Young Hak Cho
yhcho@seoultech.ac.kr

1 Graduate School of Nano IT Design Fusion, Seoul National University of Science and Technology, 232 Gongneung-ro, Nowon-gu, Seoul 01811, South Korea

2 Department of Mechanical System and Design Engineering, Seoul National University of Science and Technology, 232 Gongneung-ro, Nowon-gu, Seoul 01811, South Korea

rounded microchannels using various fabrication techniques, e.g., thermal reflow, thermal air expansion and extrusion printing. Choi et al. [7] produced microchannels with circular cross-section via soft lithography process applying the reflow phenomenon of a positive photoresist. Also, a simple fabrication process for microfluidic channels with circular cross-sectional shapes was reported using a PDMS master and thermal air expansion [8]. Xing et al. [9] fabricated rounded cross-sectional molds to cast microchannels using extrusion printing of thixotropic ink. Parekh et al. [10] fabricated a microchannel with a cross-section of semi-circular profile through direct writing with liquid metal on a substrate (e.g., PDMS) using a 3D printer. Park et al. [11] fabricated a microfluidic channel with a triangular cross-section using bulk wet etching and replica molding of PDMS to create highly defined and predictable gradients of surface-bound molecules. Furthermore, Mukherjee et al. [12] presented a simple fabrication method for low aspect-ratio triangular microchannels via micromilling and PDMS casting. Microchannels with triangular and trapezoidal cross-section were also fabricated to study inertial focusing of microparticles and manipulate them in non-rectangular cross-section channels [13, 14]. In spite of availability of all the above-mentioned geometrical cross-sections, certain challenges still exist in realizing microchannels with some geometries, particularly the parallelogram, rhombus, pentagon and hexagon.

In general, alignment including bonding is the final step in microfluidic chip fabrication. Self-alignment can be a proper tool when locating the microchips at the wanted position. Various kinds of alignment methods have been presented for self-alignment, but the main disadvantage is that some extra treatments on the microchips are necessary to realize self-alignment. Mastrangeli et al. [15] reviewed surface tension self-alignment methods and presented a broad and accessible review of the physics, material science and applications of capillary self-alignment. Kim et al. [16] utilized in situ micromechanical alignment for multilayer surface patterning using photoplastic microstencil mask.

In the present work, we have proposed a novel yet simple fabrication method of microchannels with various cross-sectional shapes, such as parallelogram, rhombus, pentagon and hexagon, which is based on the basic MEMS processes, viz. photolithography, RIE (reactive ion etching) and anisotropic KOH wet etching followed by self-alignment between Si structure and PDMS mold. We showed that the shapes of each cross-section can be controlled by the geometry of the photomask design (pattern width and interval) and the KOH etching time, and carried out experiments for confirming the inertial focusing position of particles according to the cross-sectional shape of microchannels.

2 Fabrication process

The fabrication method of microchannels of various cross-sectional shapes (such as parallelogram, rhombus, pentagon and hexagon) is briefly presented in Fig. 1. The

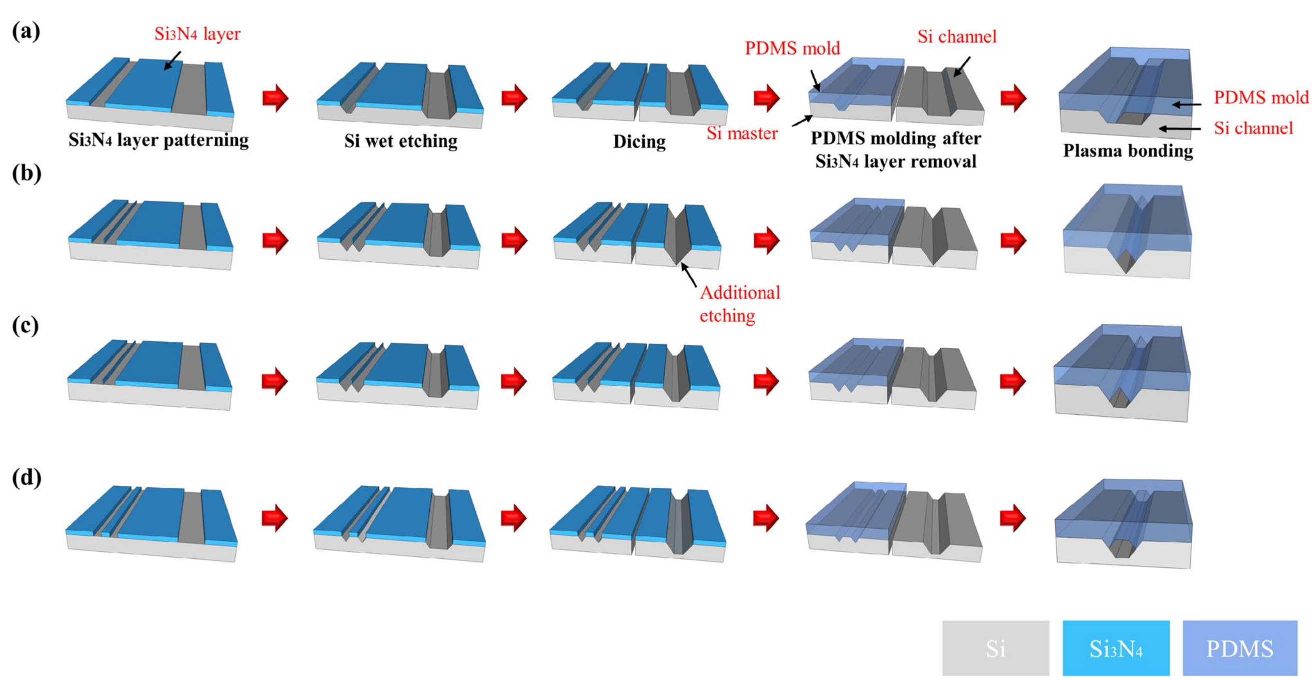

Fig. 1 Fabrication processes of microchannels with various cross-sectional shapes. **a** Parallelogram, **b** rhombus, **c** pentagon, **d** hexagon

microchannels were formed using the basic MEMS processes such as photolithography, RIE and anisotropic KOH wet etching. The common fabrication processes of the microchannels with various cross-sectional shapes are as follows: (i) Si_3N_4 thin film layer of 1000 Å thickness was deposited on (100) single crystal Si wafer using low-pressure chemical vapor deposition (LPCVD) and patterned by photolithography and RIE; (ii) the Si wafer was anisotropically etched with KOH solution at 70 °C (in case of rhombus, pentagon and hexagon channels, additional wet etching of Si microchannels was performed after dicing Si wafer); (iii) a PDMS mold was made from the Si master; (iv) the Si microchannel and the PDMS mold were self-aligned and bonded by O_2 plasma. A small amount of methanol (or DI water) was sprayed between the Si microchannel and the PDMS mold to facilitate self-alignment. Finally, the methanol was evaporated on a hot-plate to complete the formation of the microchannels which were composed of PDMS and silicon.

Previously, we already published the fabrication process of microchannel with parallelogram cross-section [17]. That method was basic and can be commonly employed for the fabrication of other kinds of microchannels. As shown in Fig. 1, the Si microchannel and master for PDMS mold for parallelogram cross-section had same etching depth unlike those for the other cross-sections (rhombus, pentagon, and hexagon). Therefore, it is possible to fabricate the Si microchannel and master in one silicon wafer without any additional etching.

The details of the relationship between the width and interval of the pattern and the cross-sectional shape of each microchannel are shown in Fig. 2. Figure shows the schematic view of the Si master for PDMS mold on the left side,

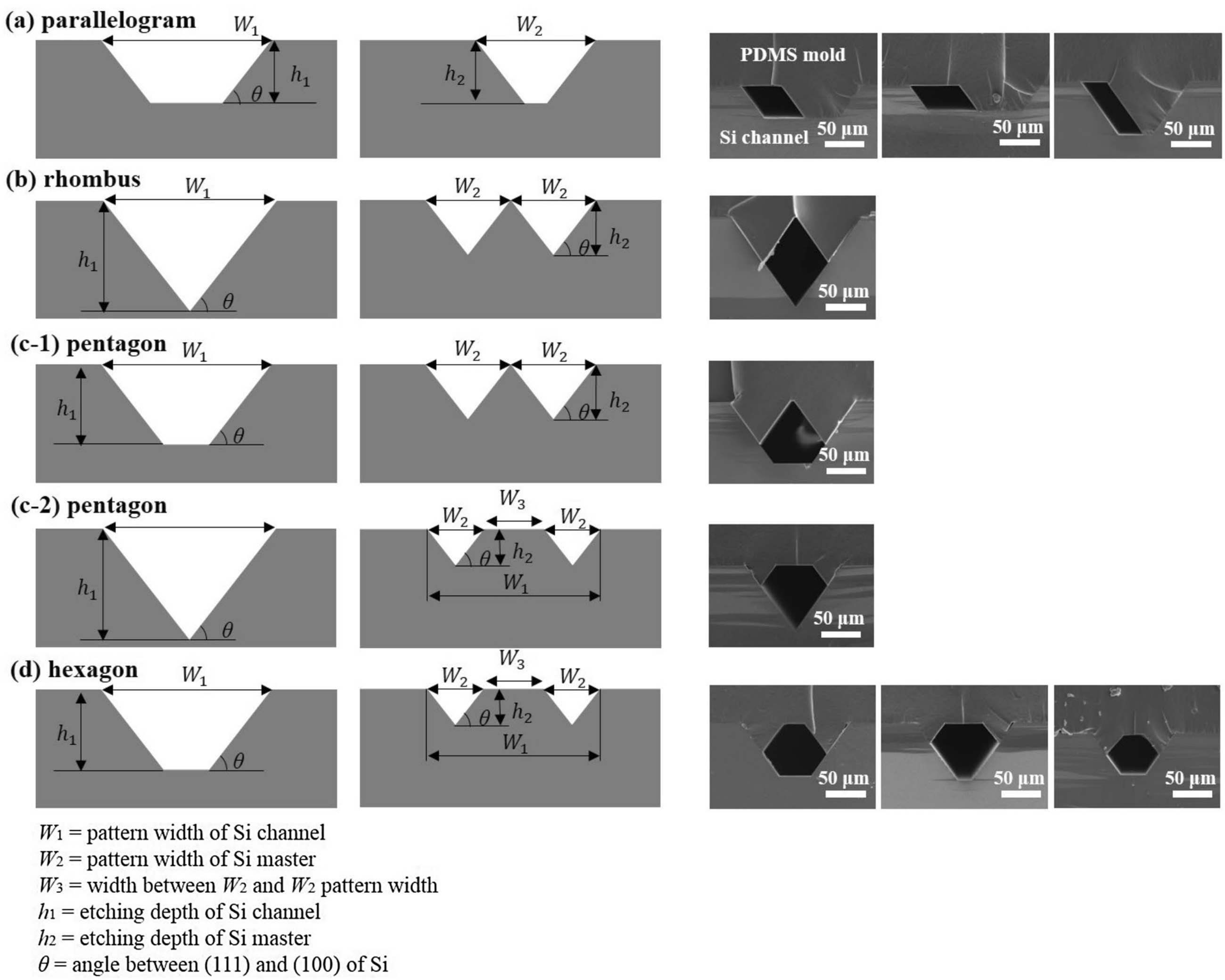

Fig. 2 Relationship between the width and interval of pattern and the cross-sectional shape of each microchannel and the SEM images. **a** Parallelogram, **b** rhombus, **c-1**, **c-2** pentagon, **d** hexagon

the Si microchannel on the right, and the scanning electron microscope (SEM) images of the fabricated microchannels

For microchannel with parallelogram cross-section (Fig. 2a), as mentioned above, Si microchannel and Si master should have the same height.

$$h_1 = h_2. \tag{1}$$

For microchannel with rhombus cross-section (Fig. 2b), the width and height of the Si microchannel should be twice as those of the Si master.

$$W_1 = 2W_2 \text{ and } h_1 = 2h_2. \tag{2}$$

Also, as shown in Fig. 2c-1, c-2, the following equations should be satisfied for microchannel with pentagon cross-section, respectively,

$$W_1 = 2W_2, \tag{3-1}$$

$$\text{or } W_1 = 2W_2 + W_3. \tag{3-2}$$

For microchannel with hexagon cross-section (Fig. 2d), the following equation should be satisfied:

$$W_1 = 2W_2 + W_3. \tag{4-1}$$

Furthermore, for microchannel with hexagon cross-section whose six sides are equal in length the following equations are satisfied:

$$h_1 = 2h_2 \quad \text{and} \quad h_2 = \left(W_1 - 2W_2\right) \sin\theta. \tag{4-2}$$

According to the relationship between $W_1 - W_2$ and h_1, we can get various shapes of parallelogram, as shown in the SEM images in Fig. 2a. The value of θ (54.7°) remains the same in all cases because it is the angle between (111) and (100) of single crystal Si. Therefore, self-alignment between Si microchannel and PDMS molds from Si master is possible because the Si microchannel and Si master were fabricated using anisotropic wet etching of Si, and therefore, they have same the crystal plane. More details will be discussed in the next section.

Figure 3 shows the SEM micrographs of representative microchannels with various cross-sectional shapes. It shows that the Si microchannel and PDMS mold were perfectly aligned and bonded because of their geometrical similarity. The cross-sectional shapes of each microchannel could be controlled by two parameters (pattern width and interval, KOH etching time), as mentioned above. The widths of the Si microchannel and PDMS mold (W_1, W_2, W_3) were determined by the widths and interval of the initial photomask design, whereas the depths of the Si microchannel and PDMS mold (h_1, h_2) were affected by the anisotropic KOH etching time. In other words, through pattern design and control of etching time, it is possible to get various types of microchannel with polygonal cross-section. In Fig. 3c, d, we obtained microchannel with hexagon cross-section with six equal sides, but no such microchannel with pentagon cross-section and having five equal sides could be formed. This was due to geometric limitation which arose because the angles of pentagon were determined by crystal direction of Si.

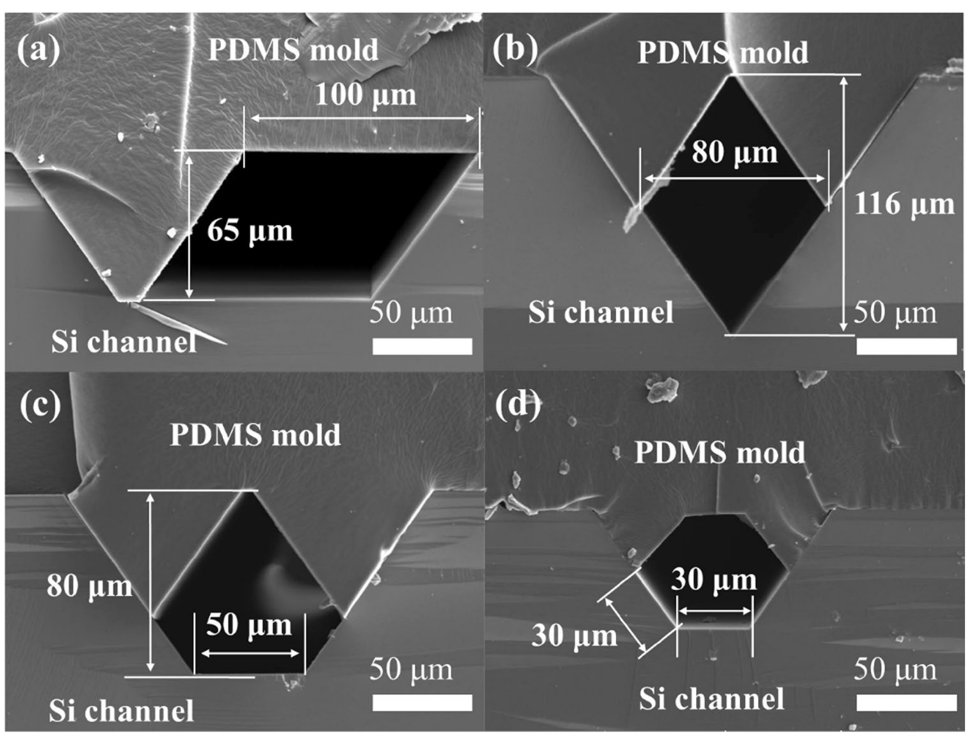

Fig. 3 SEM micrographs of microchannels with various cross-sectional shapes. **a** Parallelogram, **b** rhombus, **c** pentagon, **d** hexagon with equal sides

3 Results and discussion

Microchannels with non-rectangular cross-section have been used for specific applications such as the multilayer on-chip valves with rounded flow channels [18], haptotactic gradients of protein with triangular channels [11], and inertial focusing using half-circle and triangles [13]. In the present study, we carried out the experiments to investigate inertial focusing phenomena using the microchannels with various cross-sectional shapes. To this end, we used polystyrene particles (10 µm, green fluorescent, excitation 468 nm and emission 508 nm, Thermo SCIENCE Inc.). They were dispersed in DI water (0.05–0.1 wt% concentration) with 1% Tween 20 (Sigma-Aldrich). The particle suspensions were then injected using a syringe pump (LEGATO 111, KD Scientific Inc.) with controlled volumetric flow rate, and a fluorescence microscopy (Leica DM IL LED and Leica EL6000, Leica Microsystems Inc.) was used to confirm focusing positions in cross-sections.

According to the study by Carlo et al. [19], the channel length required for particles to reach lateral equilibrium positions (L_f) is

$$L_f = \frac{\pi \mu H^2}{\rho U_m a^2 f_L}, \tag{5}$$

where U_m is the maximum channel velocity (~1.5 U, the mean channel velocity). The average f_L was about 0.02–0.05 for channel aspect ratios (*H/W*) between 2 and 0.5, where H is the channel dimension in the direction of particle migration, W is the channel width in the perpendicular direction, μ

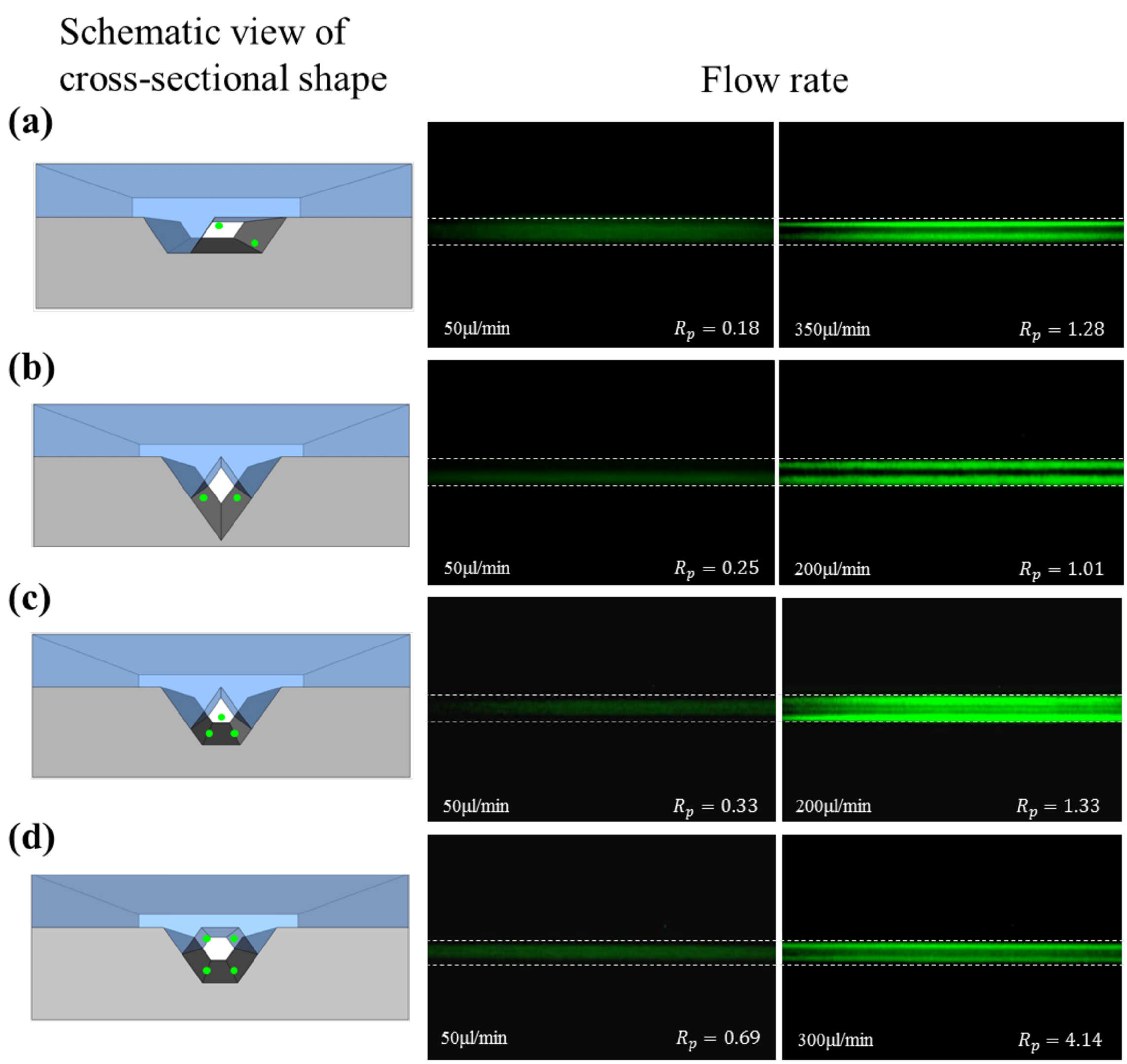

Fig. 4 Fluorescence images (top view) of inertial lift in microchannels with various cross-sectional shapes. **a** Parallelogram, **b** rhombus, **c** pentagon, **d** hexagon

and ρ are the fluid viscosity and density, and a is the particle diameter. The channel length (L_f) calculated from the parameters used in the current study using Eq. (5), was around 8.6 mm, but the fabricated channel length was 20 mm which was enough for the particles to reach lateral equilibrium. Therefore, we observed the inertial focusing at the center of the channel and near the outlet.

Figure 4 shows the fluorescent streak images from the top view according to the cross-sectional shapes. For the flow rate of 10 μl/min, there was no separation of the particles by inertial lift force. However, the inertial lift was observed when the flow rate increased (> 200 μl/min). Generally, inertial focusing position of the particles is determined by the balance of the two inertial forces (shear-gradient lift force and wall-effect lift force) [13, 19]. From the top view, we could observe several focusing positions for each microchannel. For microchannels with parallelogram and rhombus cross-sections, two focusing positions were observed, as shown in Fig. 4a, b. The focusing behavior in microchannels with parallelogram and rhombus cross-sections was very different from that in microchannel with rectangular cross-section [19]. However, they all showed the same focusing position due to their geometrical similarities (near obtuse angles of tetragon). On the other hand, three and four focusing positions were observed for microchannels with pentagon and hexagon cross-sections, respectively (Fig. 4c, d). The microchannel with pentagon cross-section showed similar focusing behavior (three focusing position) to that with triangular cross-section [13]. The difference was that there were two focusing positions in microchannel with pentagon cross-section near the bottom side, whereas in microchannel with triangular cross-section the two focusing positions were near the top side. For the hexagon with equal sides, it was difficult to observe any focusing position due to overlapped

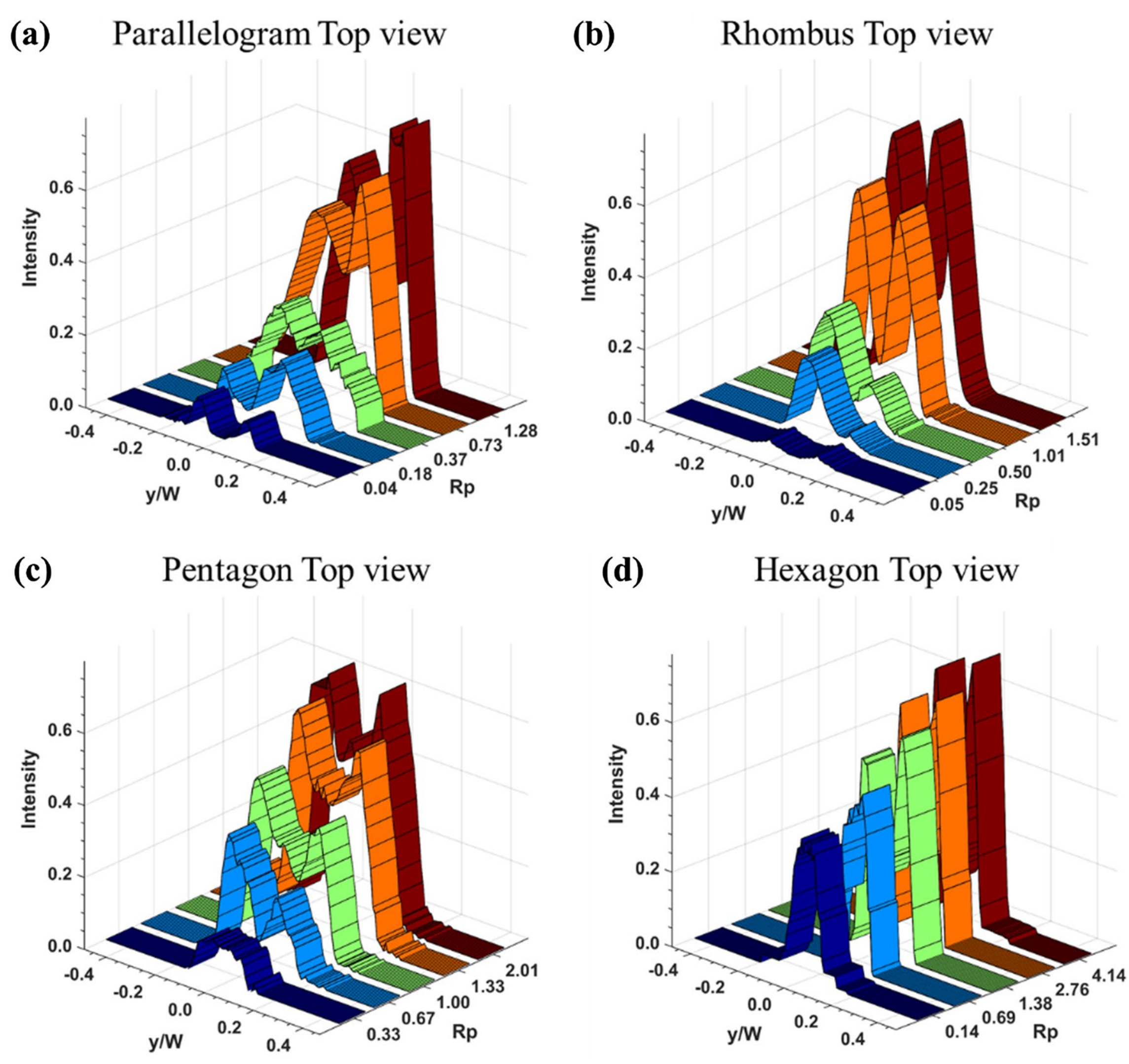

Fig. 5 Fluorescence intensities (top view) according to the particle position and R_p. **a** Parallelogram, **b** rhombus, **c** pentagon, **d** hexagon

positions, which was confirmed from confocal microscope measurement.

Two dimensionless numbers are defined to describe the flow of particles in closed channel systems [20], viz. Reynolds number (Re) and particle Reynolds number (R_p).

$$Re = \frac{\rho UD}{\mu} \quad \text{and} \quad R_p = Re\left(\frac{a}{D}\right)^2, \tag{6}$$

where ρ and μ are the density and dynamic viscosity of the fluid, respectively, U is the average velocity of the fluid, a is the particle diameter, and D is the hydraulic diameter.

We observed inertial focusing in each microchannels with varying particle Reynolds number (R_p). The normalized fluorescent intensities of particle positions in the y-coordinate are shown in Fig. 5. It shows the variation of fluorescent intensity according to particle position (y/W) and particle Reynolds number (R_p) for microchannels with cross-sections of parallelogram, rhombus, pentagon and hexagon. It clearly shows the intensity peaks that indicate the focusing positions. The particles were randomly distributed at low R_p, but with increasing R_P, the peaks representing the focusing position became clear and the positions and number of peaks agreed with the results shown in Fig. 4.

It is expected that these microchannels with various cross-sectional shapes can be a good platform to study both inertial focusing and inertial lift forces, and can be used for particle separation with high-throughput.

4 Conclusions

We used a novel yet simple process to fabricate microchannels with various cross-sectional shapes, viz. parallelogram, rhombus, pentagon and hexagon which were difficult to realize. The proposed fabrication method was based on the basic MEMS process, viz. photolithography and anisotropic wet etching. Single crystal Si wafer was used to fabricate Si microchannel and the master for PDMS mold. Microchannels with various cross-sectional shapes were easily formed through self-alignment between the Si microchannel and PDMS mold. We confirmed experimentally that the inertial focusing position of particles could be changed according to the cross-sectional shape of the microchannels.

It is expected that the fabricated microchannel with various cross-sectional shapes can be applied in wide fields such as heat transfer study in microscale, microscale transport of particle and fluid, microfluidic systems for medical and biomedical device and particle separation based on inertial focusing.

Acknowledgements This work was supported by the National Research Foundation of Korea (NRF) Grant funded by the Korean government (No. NRF-2017R1D1A1B03029817).

References

1. D.C. Duffy, J.C. McDonald, O.J.A. Schueller, G.M. Whitesides, Anal. Chem. **23**, 4974–4984 (1998)
2. L. Martynova, L.E. Locascio, M. Gaitan, G.W. Kramer, R.G. Christensen, W.A. MacCrehan, Anal. Chem. **69**, 4783–4789 (1997)
3. S. Prakash, S. Kumar, Proc. Inst. Mech. Eng. Part B J. Eng. Manuf. **229**, 1273–1288 (2015)
4. A. Tamayol, M. Bahrami, J. Fluids Eng. **132**, 111201 (2010)
5. A. Tamayol, K. Hooman, J. Fluids Eng. **133**, 091202 (2011)
6. M. Sadeghi, A. Sadeghi, M.H. Saidi, J. Fluids Eng. **138**, 031104 (2016)
7. J.S. Choi, Y. Piao, T.S. Seo, Bioprocess Biosyst. Eng. **36**, 1871–1878 (2013)
8. T.Q. Nguyen, W.-T. Park, Sens. Actuators B **235**, 302–308 (2016)
9. J. Xing, W. Rong, D. Sun, L. Wang, L. Sun, Sens. Actuators B **248**, 613–621 (2017)
10. D.P. Parekh, C. Ladd, L. Panich, K. Moussa, Lab. Chip **16**, 1812–1820 (2016)
11. J. Park, D. Kim, G. Kim, Y. Kim, E. Choi, A. Levchenko, Lab. Chip **10**, 2130–2138 (2010)
12. P. Mukherjee, X. Wang, J. Zhou, L. Papautsky, Lab. Chip **19**, 147–157 (2019)
13. J. Kim, J. Lee, C. Wu, S. Nam, D. Di Carlo, W. Lee, Lab. Chip **16**, 992–1001 (2016)
14. R. Moloudi, S. Oh, C. Yang, M.E. Warkiani, M.W. Naing, Microfluid. Nanofluid. **22**, 33 (2018)
15. M. Mastrangeli, Q. Zhou, V. Sariola, P. Lambert, Soft Matter **13**, 304–327 (2017)
16. G. Kim, B. Kim, J. Brugger, Sens. Actuators A **107**, 132–136 (2003)
17. J.Y. Kwon, D.-K. Lee, Y.H. Cho, J. Korean Soc. Precis. Eng. **36**, 287–291 (2019)
18. M.A. Unger, H.P. Chou, T. Thorsen, A. Scherer, S.R. Quake, Science **288**, 113–116 (2000)
19. H. Amini, W. Lee, D. Di Carlo, Lab. Chip **14**, 2739–2761 (2014)
20. E.S. Asmolov, J. Fluid Mech. **381**, 63–87 (1999)